

## Spin polarization vectors of field emitted electrons from Fe/W tips

T Irisawa<sup>1</sup>, T K Yamada<sup>1,2,3</sup> and T Mizoguchi<sup>1</sup>

<sup>1</sup> Faculty of Science, Gakushuin University, 1-5-1 Mejiro, Toshima, 171-8588 Tokyo, Japan

<sup>2</sup> Physikalisches Institut, Universität Karlsruhe, Wolfgang-Gaede Strasse 1, Geb.30.23, 76131 Karlsruhe, Germany

E-mail: [Toyokazu.Yamada@pi.uka.de](mailto:Toyokazu.Yamada@pi.uka.de)

*New Journal of Physics* **11** (2009) 113031 (11pp)

Received 08 July 2009

Published 17 November 2009

Online at <http://www.njp.org/>

doi:10.1088/1367-2630/11/11/113031

**Abstract.** The atomic and electronic structures at the apex of W tips were studied by means of field ion microscopy and field emission microscopy, before and after the thermal deposition of a 5 nm Fe film. Two geometries of W tip, a conventional hemi-spherical type and a chisel (flat needle) type, were prepared. The hemispherical and the chisel W tips had a  $\langle 110 \rangle$  direction parallel and perpendicular to the tip axis, respectively. The coated Fe films were found to be most likely in a non-crystalline phase, and to have a lower work function leading to a drastic change in electron emission from the apexes. The spin-polarization vectors of field-emitted electrons from these Fe/W tips were investigated with a Mott detector with a rotatable mechanism of tips. A similar absolute value of the spin-polarization vector  $|\vec{P}_{\text{tip}}| = 0.415 \pm 0.025$  was obtained for each Fe/W, while the direction of the spin-polarization vector was dependent on the shape of the apex. The angle from the tip axis was  $\theta = 45^\circ$  for the hemispherical apex and  $\theta = 66^\circ$  for the chisel apex. A spin-polarized scanning tunneling microscopy setup with a rotation mechanism of such Fe/W tips made it possible to detect both the in-plane and the out-of-plane spin component of a sample magnetization.

<sup>3</sup> Author to whom any correspondence should be addressed.

## Contents

<b>1. Introduction</b>	<b>2</b>
<b>2. Results and discussion</b>	<b>2</b>
<b>3. Conclusions</b>	<b>9</b>
<b>Acknowledgments</b>	<b>10</b>
<b>References</b>	<b>10</b>

## 1. Introduction

The field emission microscope (FEM) invented by Müller in 1936 was the first tunneling microscope [1], while the field ion microscope (FIM) invented later by him gave the first direct atomic image of tungsten (W) crystals in real space. These microscopes visualize the atomic arrangements at the apex of a sharp W tip. It is rather strange that, as far as we know, not very much information about the spin polarization of field-emitting electrons has been reported for magnetic tips; to date only for Ni tips, Fe tips, or EuS-coated W tips [2]–[6]. The apex of the tip is known to be an attractive regime since atoms at a sharp apex are not only found at the surface of the material, but exist at a singular point of the surface with less coordination, which may have unique electronic states connecting a single atom to the bulk material.

Spin-polarized scanning tunneling microscopy/spectroscopy (SP-STM/STS) is one of the techniques for investigating atomic-scale magnetism, which has been rapidly developed from the beginning of this century [7]–[30]. Magnetic images obtained with SP-STM/STS are based on a contrast, which is proportional to an inner product of the spin-polarization vector of a magnetic tip  $\vec{P}_{\text{tip}}$  and that of a sample  $\vec{P}_{\text{sample}}$  [26, 27]. In order to obtain the spin-polarization of a sample quantitatively it is essential to know the magnitude and direction of the spin-polarization vector of tunneling electrons from the tip used in the measurement. No direct measurement of the spin-polarization vector of a magnetic tip for SP-STM was reported, which limited measurement of the quantitative information from the SP-STM/STS data.

So far W tips coated with magnetic thin films are mostly used for SP-STM/STS. The most popular Fe(2–10 nm)-coated W tips are sensitive to in-plane magnetic moments of the sample surface [7]–[10], [15], [20]–[22], [25]–[32], while other kinds of tips, e.g. Cr(5–10 nm)-coated W tips, Gd(2 nm)-coated W tips and Gd<sub>90</sub>Fe<sub>10</sub>(2–3 nm)-coated W tips, have out-of-plane sensitivity at low temperatures [11, 13, 19, 23, 32]. The amplitude of the spin polarization was reported for a Fe/Al<sub>2</sub>O<sub>3</sub>/Al tunnel junction to be 0.44, which is the same for flat Fe films on W [33]. For SP-STM/STS measurements, dull tips with an apex of 1  $\mu\text{m}$  radius were reported to be appropriate [32], since there will be an almost flat apex and therefore the spin polarization vector of the Fe films follows the magnetic shape anisotropy and is aligned in-plane.

In this study, we investigated the atomic, electronic and spin structures of Fe films with a thickness of 5 nm grown on two types of W tips: (1) a conventional hemispherical type tip and (2) a chisel (flat needle) type tip by means of FIM, FEM, microbeam x-ray diffraction, scanning electron microscopy (SEM), and a custom-built instrument including a Mott detector.

## 2. Results and discussion

Two types of W tips were prepared, one by means of chemical etching from a wire, and the other from a narrow thin foil cut out perpendicularly to the roll direction. The W wires or foils

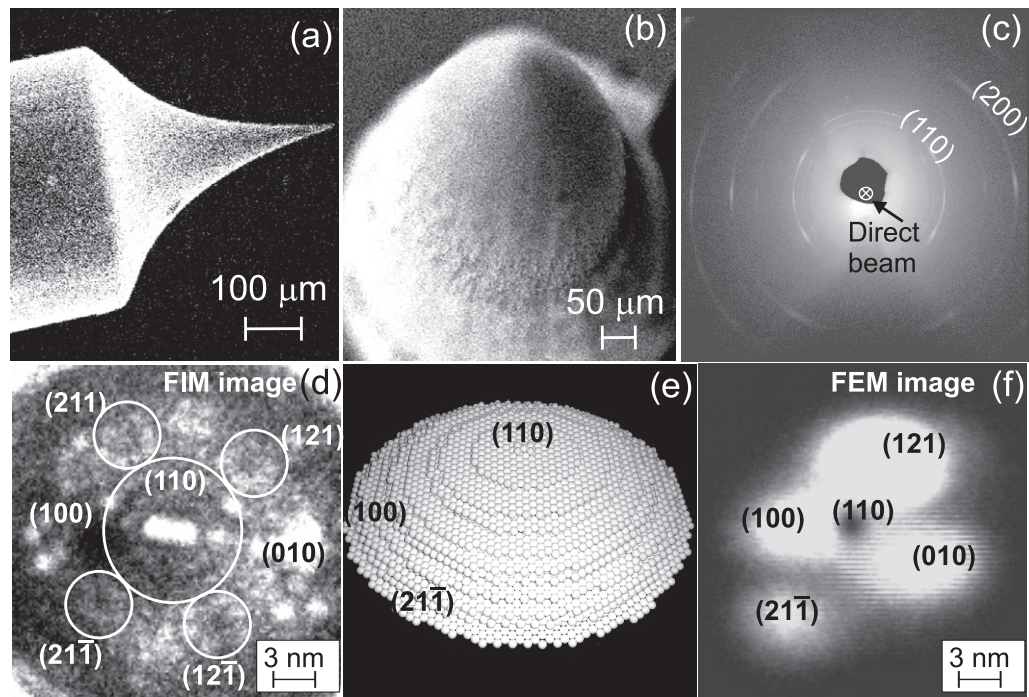


**Figure 1.** Investigations of the hemispherical W tip. (a) and (b) SEM images of the apex of the tip. A side (a) and a top (b) view. (c) X-ray Debye–Scherrer image (Cu target) obtained from the wire. (d) FIM image (+5 kV, He<sup>+</sup>). (e) Solid-sphere model. (f) FEM image (−0.4 kV).

most usually available are highly oriented polycrystals, as the slip planes of crystalline grains are parallel to the  $\langle 110 \rangle$  direction which follows the elongated direction, i.e. the wire direction or roll direction. SEM images of a hemisphere-type tip made from the wire and a chisel-type tip made from the foil are shown in figures 1(a) and (b) and 2(a)–(c), respectively. It was confirmed by x-ray diffraction measurements with a focused beam of  $5 \mu\text{m}$ , that the tip axes are parallel or perpendicular to W $\langle 110 \rangle$  at the top part of the tips, as shown in figures 1(c) and 2(d). These W tips were installed in our ultra-high vacuum (UHV) chamber and the apices of the tips were cleaned by field evaporation. The atomic structure of the obtained clean apices of the W tips was investigated by FIM.

FIM measurements were taken at room temperature in a UHV chamber ( $\sim 10^{-8}$  Pa) to investigate the atomic and electronic structures of the tip apex. He<sup>+</sup> ions of  $\sim 10^{-3}$  Pa from the apex were accelerated to a multi-channel plate (MCP) which enhanced incoming signals and showed features on a fluorescent screen imaged by a CCD camera. Single dots in the FIM image corresponded to single atoms at atomic steps. Our FIM setup had a magnification of about  $10^6$ , i.e. a 1 nm-size structure at the apex of the tip appeared as a size of 1 mm on the screen. The FIM image of the hemispherical tip is shown in figure 1(d). Concentric circles of the spots can be observed around the center of the image. The bright spot in the center of the image shows the remaining atoms in the uppermost atomic plane after the field evaporation. Our FIM measurements were taken at room temperature, and the spots are not as clear as those from an FIM operated at low temperatures. To understand the atomic structure of the tip apex, a solid sphere model was used (figure 1(e)). By comparing the model and the obtained FIM image we could identify the atomic planes around the apex of the hemispherical tip. In the center of the

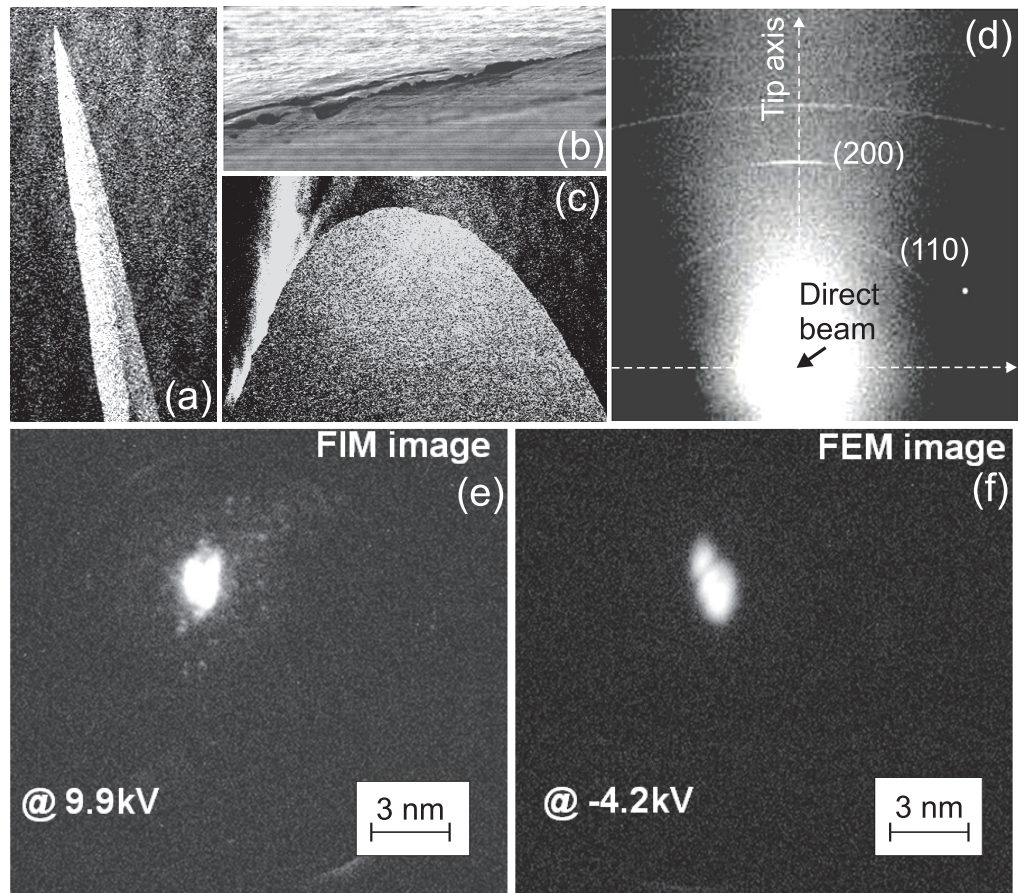


**Figure 2.** Investigations of the chisel-type W tip. (a)–(c) SEM images of the apex of the tip. Side views (a, c) and a top view (b). (d) X-ray Debye–Scherrer image (Cu target) obtained from the tip. (e) FIM image (+9.9 kV, He<sup>+</sup>). (f) FEM image (−4.2 kV).

FIM image, the area within a diameter of about 10 nm has a (110) plane. {112} and {100} atomic planes are seen around the (110) plane.

FEM measurements were performed under UHV conditions with the same experimental setup by changing the applied bias from positive to negative. In this way, we obtained the electronic structure of the same apex. The FEM image of the hemispherical tip shows four bright spots (figure 1(f)), whose positions correspond to the areas of {100} and {211} planes in the FIM image. The central plane (110), which has the highest work function [34], appears darker.

On the other hand, the chisel-type tip showed a completely different FIM image (see figure 2(e)). There were several spots in the FIM image before the tip was cleaned by the field evaporation, and only one bright spot was left after the field evaporation. Several chisel-type W tips showed the same behavior. Only bright spots instead of atomic planes were observed, which indicates a protuberance of about 3 nm at the apex. The FEM image of the same apex is shown in figure 2(f). One bright spot is observed at exactly the same position of the protuberance observed in the FIM image, i.e. electrons emit from this protuberance.

After these FIM/FEM measurements, the W tips were moved in front of an Fe evaporator in the same UHV chamber. An Fe film with a thickness of 5 nm was grown on the apex of the W tip at room temperature with an evaporation rate of  $\sim 1 \text{ nm min}^{-1}$  calibrated with a quartz

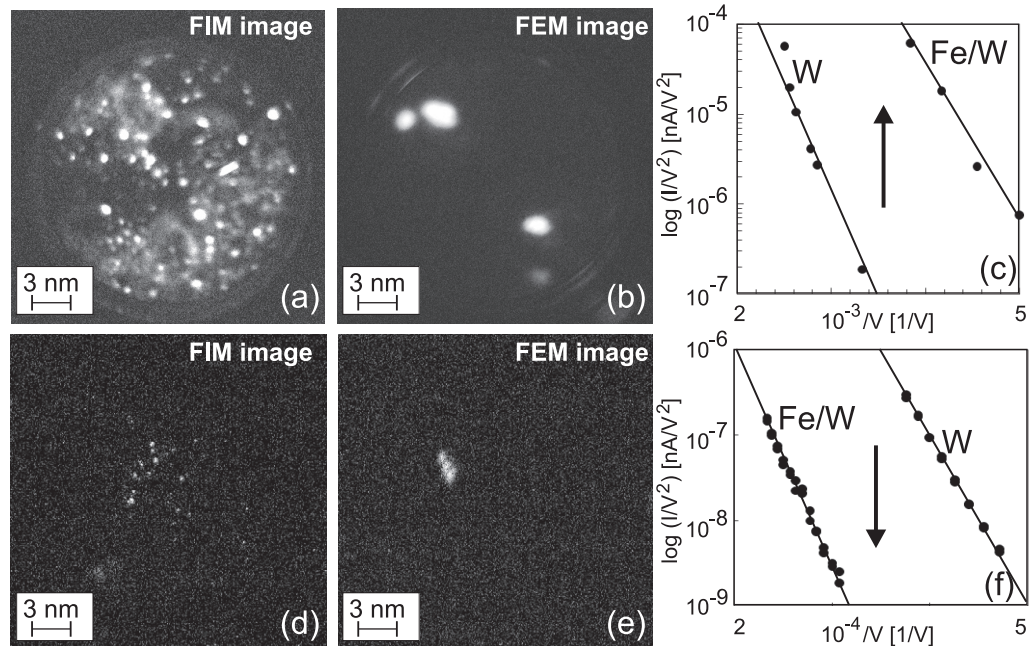


**Figure 3.** (a) and (b) show an FIM and an FEM image, respectively, obtained from the 5 nm Fe film coated on the hemisphere-type W tip. (c) F–N plot of the hemispherical W tip shifts to a lower voltage side after the deposition of a 5 nm Fe film. (d) and (e) show an FIM and an FEM image, respectively, obtained from the 5 nm Fe film coated on the chisel-type W tip. (f) F–N plot of the hemispherical W tip shifts to a higher voltage side after the deposition of a 5 nm Fe film.

thickness monitor. After the deposition, the tip was not annealed and there was no external field applied. Thus, the tips were moved back to the position for the FIM/FEM measurements.

Figure 3(a) shows the FIM image obtained from the hemispherical W tip coated by the Fe film. Many bright spots were observed, without an ordered arrangement. Also, another hemispherical W tip coated by the Fe film appeared different in FIM images, which indicates that the atomic structure of the Fe film on the hemispherical W tip with the (110) plane does not have a reproducible ordered arrangement, i.e. it probably has a non-crystalline structure. The FEM image obtained from the same apex is shown in figure 3(b). The character of the FEM image also drastically changed after the deposition of Fe (cf figure 1(f)). Four bright spots were observed around the apex, which seem not to be related to any particular atomic planes.

We took FIM/FEM measurements for the Fe-coated chisel-type W tips as well. The FIM image (figure 3(d)) shows several bright spots near the protuberance observed in the FIM image of figure 2(e). Again, no clear atomic structure was observed. Due to the curved W substrate the Fe film is not assumed to grow epitaxially, but in a non-crystalline phase. The FEM image obtained from the same apex is shown in figure 3(e). One bright spot is observed, whose position is the same as the position of the protuberance shown in figure 2(f). Electrons emit from the same position before and after the Fe deposition.

From these experiments, we conclude the following for the W tips and Fe-coated W tips. (1) The hemispherical W tip has a clean (110) plane at the apex due to the preferred

**Table 1.** Obtained parameters from the F–N plots.  $r$  denotes the radius of the tip,  $\Phi$  the work function. Details are described in the text.

	$A$	$B$ (V)	$r$ (nm)	$\Phi$ (eV)	$\alpha$	$kr$	$k\alpha$
Hemi-spherical W tip	175.1	–6265	13.4	5.84	$0.786 \times 10^8$	67.0	$3.93 \times 10^8$
Hemi-spherical Fe/W tip	192.8	–3891	18.4	3.38	$1.632 \times 10^8$	92.1	$8.16 \times 10^8$
Chisel-type W tip	1150	–48941		(5.84)		(510.1)	$(2.99 \times 10^{10})$
Chisel-type Fe/W tip	25	–56970		(3.38)		(1348.2)	$(0.45 \times 10^{10})$

$\langle 110 \rangle$  orientation parallel to the tip axis. Electrons emit mainly from the surrounding W{100} and W{211} atomic planes, while electrons emit from no clear atomic planes after the deposition of Fe. (2) The chisel-type W tip has a nanometer-scale protuberance at the apex. Electrons emit mainly from here before and after the deposition of Fe. (3) The Fe films on the hemispherical as well as the chisel-type W tips probably have a non-crystalline structure.

We measured the total electron emission curves as a function of the bias voltage by bringing a metal ball in front of the apexes of the W tips before and after the deposition of Fe (figure 3(c) for the hemispherical tip and figure 3(f) for the chisel-type tip).

The emission characteristics are expressed in the scheme of Fowler and Nordheim (F–N) [34, 38], where  $Y = \log(I/V^2)$  is plotted as a function of  $X = V^{-1}$ , as shown in figure 3(c) for hemispherical tips and in figure 3(f) for chisel-type tips. All curves are shown to be well fitted with a straight line, i.e.  $Y = A + BX$  with negative slopes ( $B < 0$ ) regardless the shape or materials at the apexes (W or Fe/W). Experimentally obtained fitted parameters  $A$  and  $B$  are summarized in table 1. From the F–N equation, those are related as  $A = \alpha/(kr)^2$  and  $B = ckr\Phi^{3/2}$ , where  $\Phi$  denotes the work function of the apex,  $k$  represents a geometric constant which is about 5 for a hemispherical apex,  $\alpha$  is proportional to a discharge area and obtained experimentally, and  $c = -0.68$  is calculated from physical constants using the unit of nm for length and nA for current.

The radius of the hemispherical W tips is estimated from the FIM image in figure 1(d) with a combination of the solid-sphere model in figure 1(e), where eight steps of the W(110) atomic planes are observed between the central (110) pole and the {211} poles. Since the angle between  $\langle 110 \rangle$  and  $\langle 211 \rangle$  is  $\cos^{-1}(3/\sqrt{12}) = 30^\circ$ , and inter-plane distance of {110} in W is  $d_{110} = 0.224$  nm, a radius of curvature of the hemisphere-type tip apex is  $r = 8d_{110}/(1 - \cos \theta) = 13.4$  nm. This value for the hemispherical W apex and the observed  $B$  value in table 1 give a work function,  $\Phi = 5.84$  eV, which is consistent with values given in the literature [34]. For a hemispherical Fe/W apex, the radius of curvature is,  $r = 18.4 (= 13.4 + 5)$  nm and the reduced  $B$  value give us the reduced work function,  $\Phi = 3.38$  eV. Thus, more emission current flows and the F–N line shifts upward.

For the chisel-type apex there is no theoretical derivation, nevertheless the F–N plots of observed data show straight lines for both the W and Fe/W apex as shown in figure 3(f). It is interesting that the F–N line for the Fe/W apex shifts downward relative to that for the W apex after deposition of Fe. If we assume the same work functions for W and Fe/W as for the hemispherical tip, the observed parameters,  $B$  and  $A(kr)^2$ , give us  $kr$  and  $k\alpha$  as shown in table 1. They are much larger than those in the hemispherical tips, suggesting the effective curvature of apex for the chisel-type tip is much larger. The apex is considered to become smoother after deposition of Fe, shifting the F–N line downward.

The spin-polarization vectors of the emission current from these Fe-coated W tips were measured by our purpose-built instrument, inclusive of a Mott detector. Field-emission electrons were mainly emitted from the Fermi level of the tip. It is certain that field-emitted electrons from the Fe-coated W tip were spin-polarized as this tip shows spin contrast in SP-STM/STS images [7]–[10], [15], [20]–[22], [25]–[32]; however, as far as we know, the spin-polarization vector has not been definitely measured so far. For a standard polarization measurement of the electron beam, a calibrated Mott detector was used [35]. It detects only components of spin-polarization perpendicular to the incident direction. In order to measure three components of the spin-polarization vector, the field-emitted electrons in the  $z$ -direction were deflected electrostatically by  $90^\circ$  without changing spin direction, as shown in figure 4(a), before going into the Mott detector, which gave a constant  $P_z$  (polarization component parallel to the tip axis) and a sinusoidal variation of  $P_y$  (polarization component perpendicular to the tip axis) as a function of the rotating angle of the tip around its axis. A schematic sketch of this system with the definition of the  $x$ -,  $y$ -, and  $z$ -axes is shown in figure 4(a). The Mott detector was calibrated using 30% spin-polarized photo-electrons from negative electron affinity (NEA)-GaAs{110} illuminated with circularly polarized light, as shown in figure 4(b). The Shaman function (the ratio of the asymmetry  $A_s$  measured with our Mott detector to the spin polarization  $P$ ) was measured to be  $S = A_s/P = 0.12$ .

Components ( $P_z$  and  $P_y$ ) of the spin-polarization vectors were obtained from the asymmetries of the measured emission current from the Fe-coated W tips with the Mott detector by rotating the tip by an angle  $\phi$  around its axis. The  $x$ ,  $y$  and  $z$  components of the spin-polarized vector are expressed in polar coordinates as  $P_x = P \sin \theta \sin \phi$ ,  $P_y = P \sin \theta \cos \phi$ , and  $P_z = P \cos \theta$ , where  $\theta$  is an angle between the polarization vector and the  $z$ -axis (the tip direction) and  $\phi$  is the angle between the polarization vector and  $y$ -axis. When we rotate the tip around the  $z$ -axis,  $P_y$  shows sinusoidal variation with the maximum value,  $P_{y:\max}$ , which is the component of the spin-polarization vector perpendicular to the tip axis. The absolute value of the vector can be obtained as  $|\vec{P}_{\text{tip}}| = \sqrt{P_{y:\max}^2 + P_z^2}$ . The direction of the spin-polarization vector of emitted electrons from the Fe-coated W tip is expressed by  $\theta = \tan^{-1}(P_{y:\max}/P_z)$  and  $\phi$  at which  $P_y$  shows the maximum value. The experimentally obtained components of the spin-polarization vector of electrons emitted from the hemispherical Fe/W apex are shown in figure 4(c). We obtain  $P_{y:\max} = 0.31$ ,  $P_z = 0.31$  and then the absolute value of the spin-polarized vector turns out to be  $|\vec{P}_{\text{tip}}| = 0.44$  and  $\theta = 45^\circ$ . The components of the spin-polarization vector of the electrons emitted from the chisel-type Fe-coated W tip are shown in figure 4(d), from which we obtain  $P_{y:\max} = 0.36$ ,  $P_z = 0.16$  and then the absolute value of the spin-polarized vector turns out to be  $|\vec{P}_{\text{tip}}| = 0.39$ ,  $\theta = 66^\circ$ , and the angle between the polarization vector and the edge direction, which is set initially in  $y$ -axis, of the chisel-type tip is  $28^\circ$ . Note that the absolute value of the spin polarization of electrons emitted from the Fe-coated W tips is  $|\vec{P}_{\text{tip}}| = 0.415 \pm 0.025$ , which is close to the value obtained for a Fe/Al<sub>2</sub>O<sub>3</sub>/Al tunnel junction [33], regardless of apex shape. With this value we can directly obtain the sample spin polarization from the experimentally obtained maximum spin contrast in SP-STM/STS data, i.e.  $|\vec{P}_{\text{sample}}| = A_{\text{STM}}/|\vec{P}_{\text{tip}}|$ .

The direction of the vector is, however, different from tip to tip, suggesting that the local direction of magnetization at the point of electron emission from an Fe film at the apex of a tip is indefinite. However, it is worth noting that an Fe/W apex, which is typically used for normal STM measurement, has an almost constant absolute value of spin-polarization vector, and has not only a perpendicular, but also a parallel component, to the tip axis for a sharp tip.

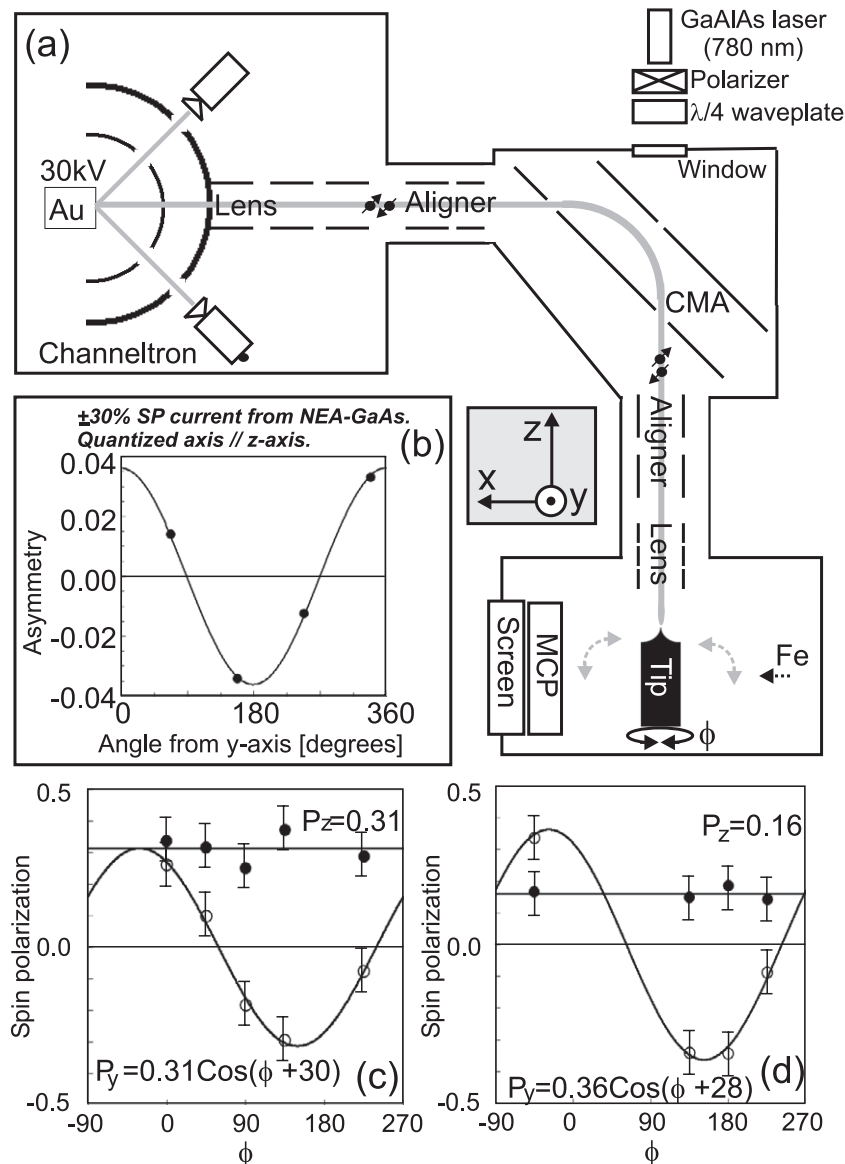


**Figure 4.** (a) Schematic sketch of our experimental setup. The gray line shows the path of the emission current beam from the apex of the tip. (b) Experimentally obtained asymmetry at each channeltron (black dots) with  $\pm 30\%$  spin-polarized current from the NEA-GaAs surface excited by a left/right circular polarized light, giving the maximum asymmetry at exactly  $0^\circ$  parallel to the  $y$ -axis. (c) and (d) Components ( $P_z$  and  $P_y$ ) of the spin-polarization vectors of field-emitted electrons from the Fe-coated W apex as a function of a rotating angle of the tip around the  $z$ -axis ( $\phi$ ). White and black dots denote experimentally obtained  $P_y$  and  $P_z$ , respectively. Plots (c) and (d) were obtained from the hemispherical tip and the chisel-type tip, respectively.

If SP-STM/STS measurements are performed with such a tip rotatable around the tip axis, all components of sample spin-polarization vector can be obtained. The amplitude of the sinusoidal variation of magnetic contrast with the tip rotation angle gives the in-plane components to



**Table 2.** Obtained values of spin polarization vectors of the Fe/W tips.

	$P_{y:\max}$	$P_z$	$ \vec{P}_{\text{tip}} $	$\theta$	$\phi$
Hemi-spherical Fe/W apex	0.31	0.31	0.44	45°	-30°
Chisel-type Fe/W apex	0.36	0.16	0.39	66°	-28°

a sample surface and the average gives the out-of-plane component. Calibration of the spin-polarization vector of the tip apex with a standard sample, e.g. Fe whiskers or photo-excited GaAs{110} cleaved in UHV [28], would be desirable for quantitative discussions.

The tips used for field emission are sharper than an ordinary SP-STM/STS tip whose apex has a radius of curvature of a few hundred nm, as described before [28, 32]. Fe thin film 5 nm thick on such a flat apex probably has in-plane magnetization, i.e.  $\theta = 90^\circ$ , and therefore in-plane sensitivity. Even in such a flat thin magnetic film, there is the possibility of magnetic domains and domain walls, which are easily identified by a slight dent or protuberance where electro-emission probably occurs. In this study sharp tips with a hemispheric or ellipsoid apex coated by Fe were used. The magnetic anisotropy, which is one of the important factors in determining domain wall width, may be weaker than that in a bulk bcc-Fe crystal since the evaporated Fe thin film on the apex of a W tip probably has a non-crystalline structure, which leads to a more gradual change of spin direction in a domain wall. Micro-magnetic simulations for magnetic domain structures of such a complex thin film have to be performed. Shape anisotropy may play an important role, as the magnetic dipole interaction is long ranged. We expected different magnetic shape anisotropies for the hemispherical apex and the chisel-type (edge-like) apex of tips.

In our previous work [26, 27] with Fe-coated W tips with a radius of about 100–200 nm, we demonstrated an in-plane sample spin polarization  $|\vec{P}_{\text{sample}}| = 0.67$  on Mn(001) surface from the observed maximum contrast of  $A_{\text{stm}} = 0.1$  by SP-STs. We required two assumptions. Firstly, that the in-plane tip and sample spin-polarization vectors were parallel and, secondly, that the amplitude of the in-plane tip spin polarization vector was 0.15, which value was estimated by a comparison between observed spin-resolved local density of states (LDOS) and theoretically calculated LDOS [26]. Now we know that the Fe-coated W tip has  $|\vec{P}_{\text{tip}}| \sim 0.415$ . With this value the angle of the polarization vector of the tip that we used can be estimated to be  $\theta = 21^\circ$ .

### 3. Conclusions

When viewing the atomic image of materials by field ion microscopy, the apex of the tip is seen to be an attractive regime since atoms at a sharp apex are not only at the surface of a solid state, but exist at a singular point of the surface with less coordination, which may have unique electronic states connecting a single atom to a solid state of materials. Iron is one of the most popular magnetic materials and many important physical properties have been found in its bulk and surface. We focused on the study of iron in the regime of the apex. There had been, to date, no direct measurement of spin-polarization vectors at the apex of magnetic tips, in spite of the fact that such magnetic tips have been widely used for SP-STM/STS, which limited the quantitative information obtainable from the experimentally obtained spin contrast in SP-STM/STS data.

In this study, we investigated the atomic, electronic and spin structures of Fe films with a thickness of 5 nm grown on the apex of the W tips. Two kinds of W tips were prepared to

study the influence of different magnetic shape anisotropy at the apex: the hemispherical W tip with a (110) plane at the apex and the chisel-type W tip (the  $\langle 110 \rangle$  direction is perpendicular to the tip axis). FIM showed that the Fe films are in non-crystalline phase. The emission of electrons from the tip was drastically changed before and after the deposition of Fe, which may be due to a great variation of the work function at the apex. All three components of the spin-polarization vector of the field-emitted electrons from Fe/W apex of two kinds of tips were measured with an instrument specially designed and constructed in-house. As shown in table 2, the absolute value of the spin-polarization vector of emitted electrons from both the hemispherical apex and the chisel-type apex were almost the same as  $|\vec{P}_{\text{tip}}| = 0.415 \pm 0.025$ , while the direction of polarization vectors was found to be different. The angle from the tip axis is  $\theta = 45^\circ$  for the hemispherical apex and  $\theta = 66^\circ$  for the chisel apex. A SP-STM setup with rotation mechanism of such Fe/W tips makes possible the detection of both in-plane and out-of-plane spin components of a sample magnetization.

### Acknowledgments

We thank Dr Hono for his advice in performing FIM experiments. We acknowledge Dr J Cole, Dr A Bork, Dr L Gerhard and Dr W Wulfhchel for their careful reading of the manuscript and for their helpful discussions.

### References

- [1] Müller E W 1937 *Z. Phys.* **106** 132
- [2] Müller N, Eckstein W, Heiland W and Zinn W 1972 *Phys. Rev. Lett.* **29** 1651
- [3] Chrobok G, Hofmann M, Regenfus G and Sizmann R 1977 *Phys. Rev. B* **15** 429
- [4] Landolt M and Campagna M 1977 *Phys. Rev. Lett.* **38** 663  
Landolt M and Campagna M 1978 *Surf. Sci.* **70** 197
- [5] Landolt M and Yafet Y 1978 *Phys. Rev. Lett.* **40** 1401
- [6] Nagai S, Fujiwara Y and Hata K 2009 *Ultramicroscopy* **109** 395
- [7] Wiesendanger R, Bode M and Getzlaff M 1999 *Appl. Phys. Lett.* **75** 124
- [8] Heinze S, Bode M, Kubetzka A, Pietzsch O, Nie X, Blügel S and Wiesendanger R 2000 *Science* **288** 1805
- [9] Kleiber M, Bode M, Ravlić R and Wiesendanger R 2000 *Phys. Rev. Lett.* **85** 4606
- [10] Pietzsch O, Kubetzka A, Bode M and Wiesendanger R 2001 *Science* **292** 2053
- [11] Krause S, Berbil-Bautista L, Herzog G, Bode M and Wiesendanger R 2007 *Science* **317** 1537
- [12] Bode M, Heide M, von Bergmann K, Ferriani P, Heinze S, Bihlmayer G, Kubetzka A, Pietzsch O, Blügel S and Wiesendanger R 2007 *Nature* **447** 190
- [13] Meier F, Zhou L, Wiebe J and Wiesendanger R 2008 *Science* **320** 82
- [14] Wulfhchel W, Ding H F, Lutzke W, Steierl G, Vazquez M, Marin P, Hernando A and Kirschner J 2001 *Appl. Phys. A* **72** 463
- [15] Yamasaki A, Wulfhchel W, Hertel R, Suga S and Kirschner J 2003 *Phys. Rev. Lett.* **91** 127201
- [16] Schlickum U, Wulfhchel W and Kirschner J 2003 *Appl. Phys. Lett.* **83** 2016
- [17] Schlickum U, Janke-Gilman N, Wulfhchel W and Kirschner J 2004 *Phys. Rev. Lett.* **92** 107203
- [18] Gao C L, Schlickum U, Wulfhchel W and Kirschner J 2007 *Phys. Rev. Lett.* **98** 107203
- [19] Gao C L, Wulfhchel W and Kirschner J 2008 *Phys. Rev. Lett.* **101** 267205
- [20] Yang H, Smith A R, Prikhodko M and Lambrecht W R L 2002 *Phys. Rev. Lett.* **89** 226101
- [21] Okuno S N, Kishi T and Tanaka K 2002 *Phys. Rev. Lett.* **88** 066803
- [22] Kawagoe T, Iguchi Y, Yamasaki A, Suzuki Y, Koike K and Suga S 2005 *Phys. Rev. B* **71** 014427

- [23] Yayon Y, Brar V W, Senapati L, Erwin S C and Crommie M F 2007 *Phys. Rev. Lett.* **99** 067202
- [24] Prokop J, Kukunin A and Elmers H J 2006 *Phys. Rev. B* **73** 014428
- [25] Yamada T K, Bischoff M M J, Mizoguchi T and van Kempen H 2003 *Appl. Phys. Lett.* **82** 1437
- [26] Yamada T K, Bischoff M M J, Heijnen G M M, Mizoguchi T and van Kempen H 2003 *Japan. J. Appl. Phys.* **42** 4688
- [27] Yamada T K, Bischoff M M J, Heijnen G M M, Mizoguchi T and van Kempen H 2003 *Phys. Rev. Lett.* **90** 056803
- [28] Matsuda T, Tonomura A, Yamada T K, Okuyama D, Mizuno N, Vazquez de Parga A L, van Kempen H and Mizoguchi T 2005 *IEEE Trans. Magn.* **41** 3727
- [29] Yamada T K, Robles R, Martinez E, Bischoff M M J, Vega A, Vazquez de Parga A L, Mizoguchi T and van Kempen H 2005 *Phys. Rev. B* **72** 014410
- [30] Yamada T K, Martinez E, Vega A, Robles R, Stoeffler D, Vazquez de Parga A L, Mizoguchi T and van Kempen H 2007 *Nanotechnology* **18** 235702
- [31] Balashov T, Takacs A F, Wulfhekel W and Kirschner J 2006 *Phys. Rev. Lett.* **97** 187201
- [32] Bode M 2003 *Rep. Prog. Phys.* **66** 523
- [33] Tedrow P M and Meservey R 1973 *Phys. Rev. B* **7** 318
- [34] van Tol M F H, Hondsmerk F A, Bekker J W and Nieuwenhuys B E 1992 *Surf. Sci.* **266** 529
- [35] Oshima Y, Yamada T, Fujii J and Mizoguchi T 2001 *Trans. Magn. Soc. Japan* **1** 16
- [36] Dyke W P, Trolan J K, Dolan W W and Barnes G 1953 *J. Appl. Phys.* **24** 570
- [37] Pierce D T and Meier F 1976 *Phys. Rev. B* **13** 55484  
Pierce D T, Celotta R J, Wang G C, Unertl W N, Galejs A, Kuyatt C E and Mielczarek S R 1980 *Rev. Sci. Instrum.* **51** 478
- [38] Fowler R H and Nordheim L W 1928 *Proc. R. Soc. Lond. A* **119** 173